Polarized Surface Enhanced Raman and Absorbance Spectra of Aligned Silver Nanorod Arrays

Y.-P. Zhao,*,† Stephen B. Chaney,† Saratchandra Shanmukh,‡ and Richard A. Dluhy‡

Nanoscale Science and Engineering Center, Department of Physics and Astronomy, and Department of Chemistry, University of Georgia, Athens, Georgia 30602

Received: December 20, 2005

Polarized surface-enhanced Raman scattering (SERS) and UV−vis absorbance spectra were measured for a nonplanar Ag nanorod array substrate prepared by oblique angle vapor deposition. The anisotropy of the SERS polarization was shown to differ from that of the polarized UV−vis absorbance. The maximum SERS intensity was observed in the polarization direction perpendicular to the long axis of the Ag nanorods, while the UV−vis absorbance was strongly polarized along the direction of the long axis of the nanorod array. Analysis of the polarization data showed that molecular orientation was not the cause of the anisotropic SERS scattering. Rather, the SERS anisotropy was primarily attributed to the lateral arrangement of the three-dimensional tilted nanorod lattice in which highly localized plasmon modes are created by strong electromagnetic coupling between adjacent metallic nanorods.

Introduction

The polarization dependence of the surface-enhanced Raman spectroscopy (SERS) effect has recently been investigated for several different nanostructured substrates, including nanoparticle dimers,[1] nanoparticle aggregates,[2−4] regular arrays of nanospheriods,[5] aligned nanowire bundles,[6,7] scratched metal surfaces,[8,9] and Y-junctions.[10] For isolated nanoparticle aggregates or small arrays, the anisotropic polarized SERS signals are consistent with the topological anisotropy of the nanostructures,[1−5] i.e., stronger SERS signals appear along the long axis of the nanoparticles. These studies generally take advantage of the plasmon-resonant condition, i.e., the situation where the Raman laser excitation wavelength is at, or close to, the electronic plasmon resonance peak of the nanoparticles. For example, recent work by Grand, et al. showed excellent phase agreement between the normalized SERS intensity and normalized extinction intensity at the excitation wavelength for a regular array of spheroid nanoparticles.[5]

The current theoretical understanding of SERS attributes its enhanced intensity to the local electric fields in a confined geometry where the probe molecules are located,

$$I_{\mathrm{SERS}} \propto \left|\frac{E_{\mathrm{local}}(\omega_0)}{E_0(\omega_0)}\right|^2 \left|\frac{E_{\mathrm{local}}(\omega_s)}{E_0(\omega_s)}\right|^2 \approx \left|\frac{E_{\mathrm{local}}(\omega_0)}{E_0(\omega_0)}\right|^4 \qquad (1)$$

where $E_{\mathrm{local}}(\omega_0)$ and $E_{\mathrm{local}}(\omega_s)$ are the enhanced local electric fields at the incident and scattered frequencies, and $E_0(\omega_0)$ and $E_0(\omega_s)$ are the incident fields. The approximation in eq 1 is due to the fact that the Raman-shift wavelength is very small compared to the incident wavelength. For resonant SERS, only the electric field along the long axis of the nanoparticle can excite the plasmon resonance, implying that $E_{\mathrm{local}}(\omega_0) \propto E_0(\omega_0) \cos\theta$. Thus, $I_{\mathrm{SERS}} \propto \cos^4\theta$, where θ is the polarization angle with respect to the long axis of the anisotropic object. This relationship has been experimentally demonstrated.[1−5]

A strong SERS polarization dependence has also been observed in aligned aggregates of high-aspect-ratio nanowires or nanorods.[6−11] Unlike the case of isolated nanoparticles, however, the maximum SERS intensity observed for these assemblies of elongated nanoparticles is in the polarization direction perpendicular to the long axis of the rods/wires. Both $\cos^2\theta$ and $\cos^4\theta$ functions have been used to fit the SERS intensity profiles in these systems.[6,7] Because of their high aspect ratio, the transverse mode (TM) of the plasmon resonance in the nanorods and nanowires is generally blue-shifted to below 400 nm, while the longitudinal mode (LM) of the resonant wavelength is red-shifted to above 1000 nm. Because the Raman laser excitation wavelength in these studies is between 500 and 800 nm, the anisotropic SERS polarization response for these nanorod and nanowire ensembles occurs under nonplasmon-resonance conditions.

Perpendicularly polarized SERS in elongated nanoassemblies may also be observed under resonance conditions. Tao et al. demonstrated that an anisotropic SERS response with a preferred polarization direction perpendicular to the long axis of a nanowire aggregate also occurs when there is high absorbance at the excitation wavelength.[7,12] The large SERS enhancement in this case was attributed to either a plasmon mode in the gap between two rods or a multimode plasmon resonance.[7] In most studies, however, the connection between the SERS anisotropy and the optical absorbance for the same substrate has not been well investigated, and the mechanism of nonplasmon-resonance SERS is still controversial.

Recently, we discovered that a nonplanar Ag nanorod array fabricated by an oblique angle deposition method exhibited extremely high SERS enhancements.[13] The enhancement mechanism was attributed to the high aspect ratio and anisotropic nature of the substrate.[11] In this report, we present a detailed study of the polarized SERS response of this nonplanar Ag nanorod ensemble with a very high aspect ratio. We show that the SERS polarization anisotropy differs from that of the

* Corresponding author. E-mail: zhaoy@physast.uga.edu.
† Department of Physics and Astronomy.
‡ Department of Chemistry.

10.1021/jp057406o CCC: $33.50 © 2006 American Chemical Society
Published on Web 01/27/2006

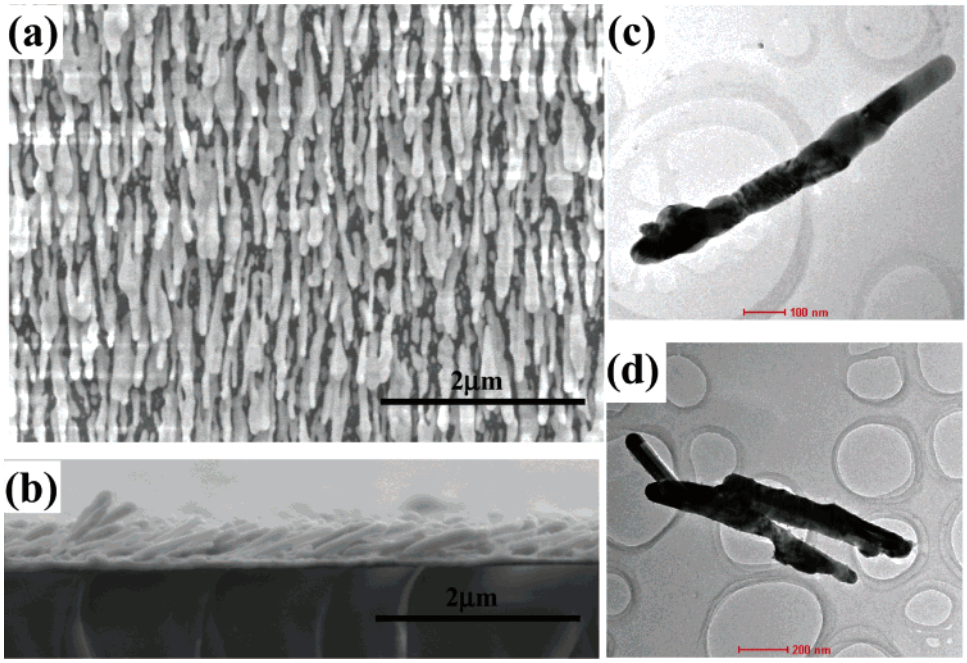

Figure 1. (a) Top view and (b) the cross-sectional view SEM images of the Ag nanorod array on a glass slide. The scale bars represent 2 μm. The top view SEM was measured without additional metallic coating. (c and d) Representative TEM images of the individual Ag nanorods. Scale bar is: (c) 100 nm, (d) 200 nm.

polarized UV−vis−NIR absorbance anisotropy for the same substrate and that the mechanisms for the SERS enhancement along and perpendicular to the nanorods are different.

Experimental Methods

The Ag nanorod arrays were prepared by an oblique-angle vapor deposition (OAD) technique, as reported earlier.[13] In the current study, the Ag nanorod array was directly deposited onto a bare glass slide in order to obtain both SERS and optical absorption spectra on the same substrate. Figure 1 shows the top view and cross-section SEM images of the nanorod array as well as some representative TEM images of individual nanorods detached from the substrate by sonication in H_2O. The Ag nanorods resulting from OAD on the glass slides were aligned parallel to each other at an angle of 71.3 ± 4° with respect to the substrate surface normal. The silver rods had an average length of 868 ± 95 nm and an average diameter of 99 ± 29 nm. The average gap between two rods was approximately 177 nm, resulting in a density of 13.1 ± 0.5 rods/μm^2. Both SEM and TEM images demonstrated that the rods were not perfectly cylindrically shaped. Rather, the vapor deposition process resulted in irregularly shaped cylinders with corrugations, needles, and bifurcations of the nanorods, see, e.g., Figure 1c and 1d.

The SERS measurement was performed by using a fiber-optic-coupled, confocal Raman microscope interfaced to a CCD-equipped spectrograph (Kaiser Optical, Inc., Ann Arbor, MI). A fiber-optic-interfaced 785-nm near-IR diode laser (Invictus, Kaiser Optical) was used to provide the incoming radiation. The Raman probe head was modified for polarization studies by first polarizing the incoming laser beam using a Glan−Thompson prism linear polarizer (Karl Lambrecht, Chicago, IL). A broadband half-wave plate (Karl Lambrecht) was then used to tune the state of polarization of the incident beam. Polarization-dependent SERS spectra were recorded by rotating the half-wave plate by increments of 10°, thereby changing the polarization angle θ between the incoming electric field and the long axis of the nanorods. For convenience, we define

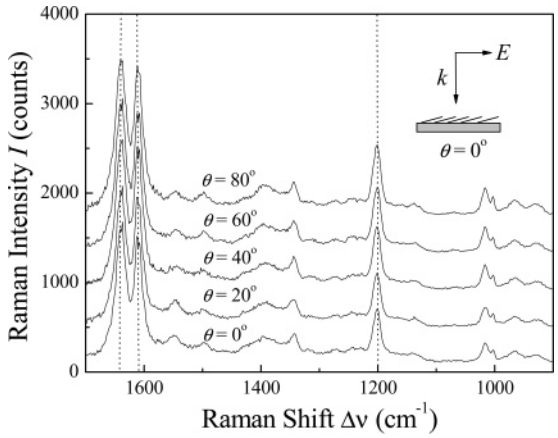

Figure 2. Polarized SERS spectra of BPE on the Ag nanrod substrates as a function of the incoming polarization angle. The diagram shows the *p*-polarization direction (θ = 0°).

p-polarization as the direction of the incident electric field that is parallel to the major long axis of the nanorods (θ = 0°) and *s*-polarization as the direction of the incident field that is perpendicular to the long axis of the nanorods (θ = 90°). The molecular probe used in this study was *trans*-1,2-bis(4-pyridyl)-ethene (BPE, Aldrich, 99.9+%). The incident laser beam was delivered to the sample by epi-illumination through a 50× microscope objective. SERS spectra were collected from multiple spots on the substrate by 180° backscattering through the same microscope objective used to deliver the incident light.

Results and Discussion

Polarized SERS of BPE on Aligned Ag Nanorod Arrays. Figure 2a shows the polarization-dependent SERS spectra of BPE on the Ag nanorod array. The intensity of all the major bands in this figure increased when the polarization angle θ changed from 0° to 80°. To better illustrate the anisotropic nature of the SERS polarization response, the integrated intensities of three major BPE Raman bands, i.e., 1200 cm^{-1} (in-plane ring

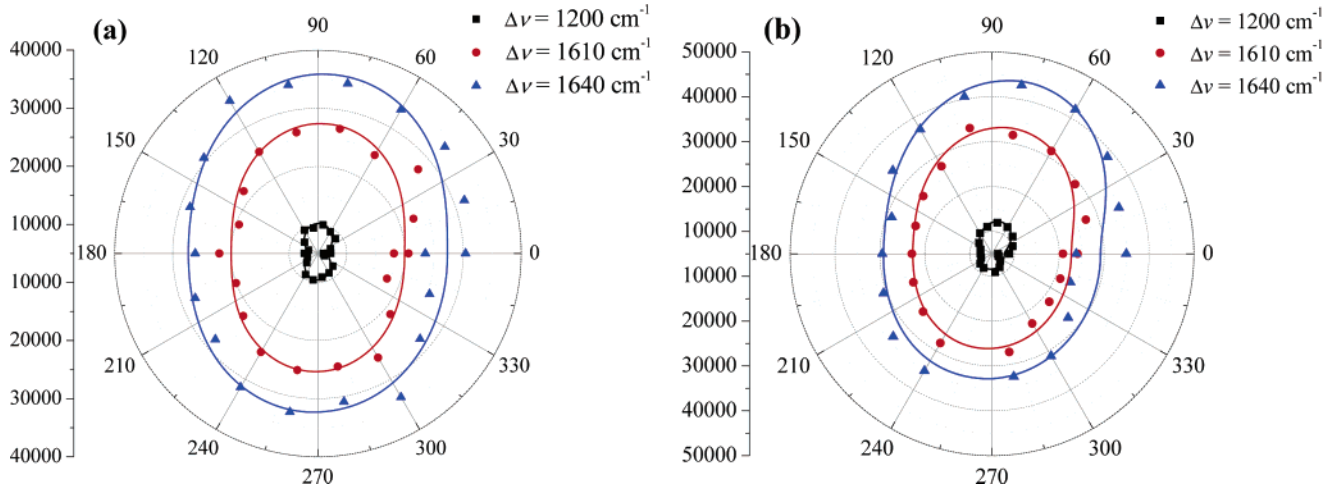

Figure 3. Polar plots of the integrated intensities of the 1200, 1610, and 1640 cm^{-1} Raman bands of BPE at two different locations on the substrate. The solid curves are the fittings according to the equation in the text. (a) Plot of the band intensities obtained from the spectra presented in Figure 2. The ellipticities for the three bands in (a) are 1.25, 1.20, and 1.20, while the ellipticities in (b) are 2.56, 1.81, and 2.0.

mode), 1610 cm^{-1} (pyridine ring C═C stretching mode), and 1640 cm^{-1} (C═C stretching mode),[14] were plotted using polar coordinates, as shown in Figure 3a. For all three Raman bands, the maximum intensities occurred at *s*-polarization ($\theta = 90°$ or 270°), while the minimum intensities occurred at *p*-polarization ($\theta = 0°$ or 180°). Figure 3a shows that the absolute band intensities are different for the three Raman bands. However, the anisotropic shape of the polarization-dependent SERS response is similar in each case. For each band, the minimum intensity is approximately 0.8 that of the maximum intensity. In addition, the contour of this anisotropic polarization response is conserved across the entire substrate. Figure 3b illustrates the integrated intensities of the three Raman bands obtained from spectra acquired at a separate location on the substrate. While the band intensities at this location differ slightly from those plotted in Figure 3a, the anisotropic polarization profile is similar for the two spots.

The SEM images indicate that the nanorod array is tilted at an angle of ~71.3° with respect to the surface normal. Therefore, the incident *p*-polarized electric field E_{p0} is not completely parallel to the rods. Rather, there is a small additional *s*-component, $E^s_{p0} = E_{p0} \cos 71.3° = 0.32E_{p0}$. Equation 1 can be used to explain the experimental data in Figure 3 if one assumes that both *p*- and *s*-polarizations induced a SERS response of different strengths, or in other words, if there are different local field enhancements α_p and α_s for the two polarization directions. In this case, the overall field enhancement can be written as $|E_{local}(\omega_0)|^2 \propto |E_0(\omega_0)|^2(\alpha_p^2 \cos^2\theta + \alpha_s^2 \sin^2\theta)$. According to eq 1, $I_{SERS} \propto (1 + A \sin^2\theta)^2$, where $A = (\alpha_s^2 - \alpha_p^2)/\alpha_p^2$ is characteristic of the anisotropy of the local *E*-field relative to the major axis.

We observed that the band intensities in the BPE SERS spectra decayed after multiple measurements on the same spot, presumably due to sample bleaching induced by the incident laser. To account for this bleaching effect in the data analysis, we used a function, $I = I_0(1 + A\, e^{-\theta/\theta_0} \sin^2\theta)^2$, to fit the SERS intensities. In this expression, the exponential decay was used to describe the bleaching-induced intensity decrease. This function produced a good fit with the experimental data and was used in the curve fitting of the polarization anisotropy plots for the BPE bands shown in Figure 3. The results of the fit gave a value of $A \sim 0.095-0.6$ and an ellipticity $[= (1 + A)^2]$ of the SERS anisotropy of between ~1.2 − 2.56.

One possible explanation for the *s*-polarized SERS anisotropy of BPE on these nanorod arrays involves the preferred orientation of this probe molecule on the surface. BPE is a long, centrosymmetric molecule that preferentially orients with its long axis perpendicular to a Ag substrate.[14,15] Inspection of the Ag nanorod array geometry (Figure 1) reveals that alignment of BPE molecules perpendicular to the long axis of the nanorod would orient the long axis of BPE along the *s*-polarized geometric direction, leading to an increased SERS response for that polarization. In addition, theoretical calculations show that the polarized SERS intensity for BPE should be anisotropic, with a minimum intensity observed at the point where the incident *E*-field is perpendicular to the long axis of the BPE molecule.[14] These calculations predict that a minimum SERS intensity should occur for BPE in the *p*-polarized geometric direction on the Ag nanorod array, which is the situation observed experimentally (Figure 3).

We have tested the hypothesis that a preferred molecular orientation of BPE is the cause of the observed SERS anisotropy by using a spectroscopic ratio to characterize the orientation of the BPE molecule on the Ag nanorods. This method utilizes the intensity ratio of the 1610 and 1640 cm^{-1} BPE vibrations to the one at 1200 cm^{-1}. The I_{1640}/I_{1200} and I_{1610}/I_{1200} ratios should be representative of molecular direction because the 1610 and 1640 cm^{-1} BPE vibrations have been found to be sensitive to molecular orientation, while the 1200 cm^{-1} band is less so.[14,15] Figure 4 plots the SERS intensity ratios I_{1640}/I_{1200} and I_{1610}/I_{1200} as a function of the incoming polarization angle for two different locations on the Ag nanorod array substrate. The intensity ratio curves in Figure 4 were calculated by using the data from Figure 3.

The normalized SERS intensity ratios I_{1640}/I_{1200} and I_{1610}/I_{1200} have the effect of (i) minimizing the anisotropic contribution of the substrate, and (ii) enhancing any anisotropic contribution due to molecular orientation. The data plotted in both Figure 4a and b show a marked lack of preference to the incoming polarization direction in the I_{1640}/I_{1200} and I_{1610}/I_{1200} orientation ratios. While the ratios in Figure 4a show a slight deviation from isotropic behavior, the ratios in Figure 4b are isotropic in nature. For both sampling locations, we conclude that there is no pronounced preferred molecular orientation of BPE on the Ag nanorod array. Statistically, when SERS spectra are acquired at multiple locations over the entire nanorod substrate, the I_{1640}/I_{1200} and I_{1610}/I_{1200} intensity ratios are

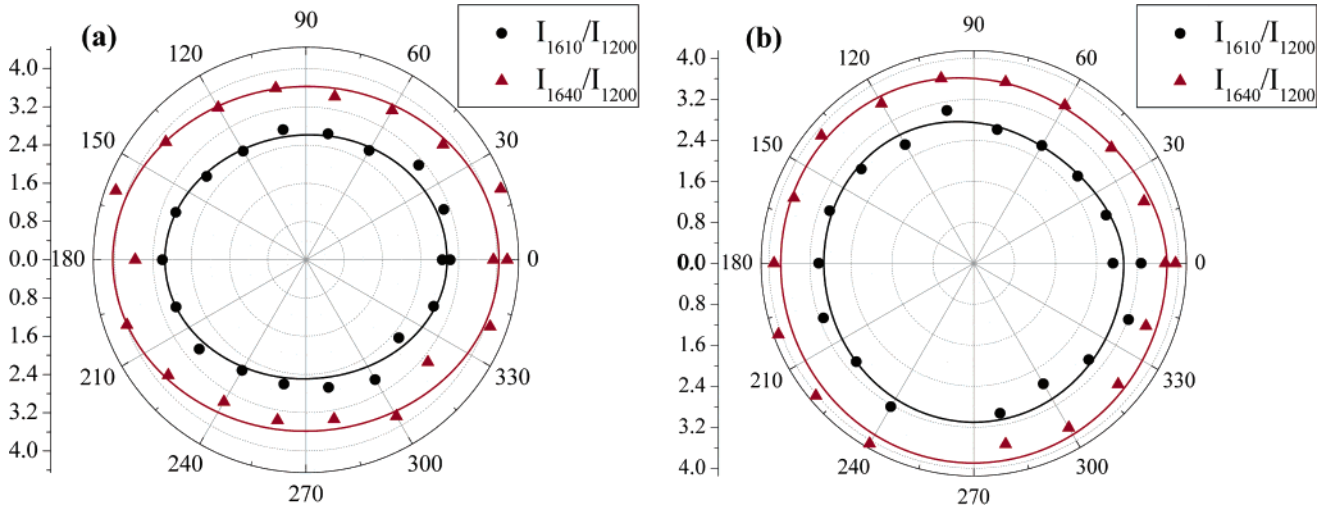

Figure 4. Polar plots of the intensity ratios I_{1640}/I_{1200} and I_{1610}/I_{1200} obtained from the BPE Raman bands at 1640, 1610, and 1200 cm^{-1}. Intensity ratios plotted vs the polarization angle for two different substrate locations. The plots in Figure 4 were calculated by using the data from Figure 3.

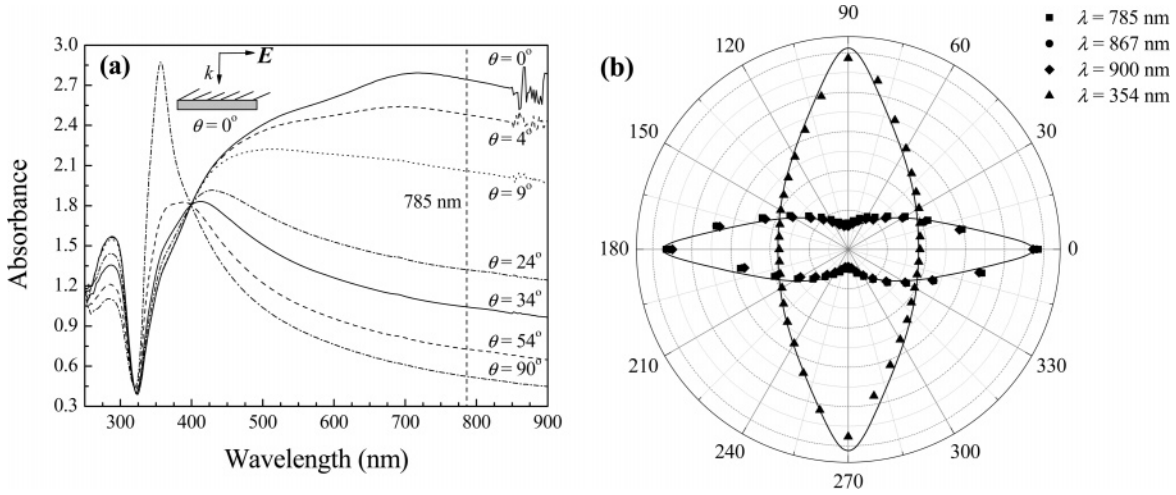

Figure 5. (a) Polarized UV−vis−NIR absorption spectra of the Ag nanorod substrates. The diagram shows the *p*-polarization direction ($\theta = 0°$); (b) Polar plots of the absorbance at $\lambda = 785$, 867, 900, and 354 nm, respectively. The solid curves are the fittings according to the equation in the text.

consistent with the data shown in Figure 4, giving no indication of preferred molecular orientation. We, therefore, conclude that the molecular orientation of BPE is not the underlying cause for the SERS anisotropy measured for these Ag nanorod arrays.

Polarized UV−Vis−NIR Absorbance of Aligned Ag Nanorod Arrays. The polarized UV−vis absorption spectra of the same Ag nanorod substrate used in the SERS experiments were measured by a UV−vis−NIR double-beam spectrophotometer (JASCO V-570). The spectrophotometer was modified by placing two rotatable polarizers in the paths of the incident beams to obtain the polarized absorption spectra. Figure 5a shows the polarization-dependent absorbance spectra for a ~867-nm long Ag nanorod substrate. For *p*-polarization ($\theta = 0°$), a broad absorption feature appears at vis wavelengths above 400 nm. When the polarization angle θ is rotated toward *s*-polarization ($\theta = 90°$), the absorbance of the broad vis contour steadily decreases, while a sharp UV peak emerges at 357 nm. This sharp peak is attributed to the transverse plasmon mode of the nanorod array.

The 785-nm Raman excitation wavelength used in the SERS experiments is shown by the dashed line in Figure 5b. This 785-nm wavelength is within the broad vis−NIR absorbance contour prominent in *p*-polarization, however, the absorbance at 785 nm decreases dramatically as the polarization rotates from *p* to *s*. The polar contour plots corresponding to the TM plasmon peak at $\lambda = 354$ nm as well as the wavelengths $\lambda = 785$, 867, and 900 nm within the broad vis−NIR absorbance contour are shown in Figure 5b. The wavelengths $\lambda = 867$ nm and $\lambda = 900$ nm correspond to the wavelengths of the Stokes-shifted 1200 and 1640 cm^{-1} Raman bands, respectively. Because the Raman shift is small, the absorbance plots of $\lambda = 785$, 867, and 900 nm were collapsed together.

Figure 5b shows that the polar contour plot of the TM plasmon peak at $\lambda = 354$ nm has a 90° phase shift with respect to the plots at $\lambda = 785$, 867, and 900 nm. The fitting function used to describe the anisotropic absorbance data in Figure 5b was $AB = -\beta \ln[\eta(1 + B \sin^2 \theta)]$, where $\beta = 1$ for an isotropic medium, and $\beta \neq 1$ for an anisotropic medium due to induced cross-polarization. The ellipticity of the absorbance data at 785, 867, and 900 nm was ~8.4, while the ellipticity for the absorbance at 354 nm was 2.85.

The ellipticity of the absorbance at 785 nm is very close to the aspect ratio of the nanorods (~8.8) and is much greater than the ellipticity of the SERS intensity (~1.2−2.56). According to the optical theorem,[16] the extinction depends on the scattering far field amplitude in the forward direction. If eq 1 is valid in this instance, the SERS signal predominately reflects the local electric field from the scattering of a SERS-active particle.

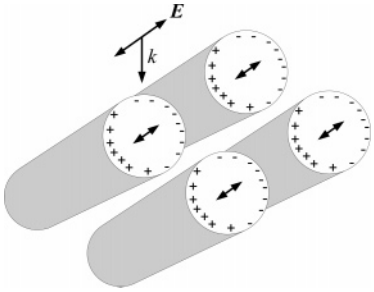

Figure 6. The proposed dipole arrangement in the Ag nanorod array under *s*-polarization excitation.

A Model for Polarized SERS in Aligned Ag Nanorod Arrays. The anisotropic SERS local field can be explained by the entrapment of the *s*-polarized fields in cavities between the nanorods. In the case of these Ag nanorods, the ensemble nature of the substrate restricts the *s*-polarized local field within a confined geometry. Theoretical calculations[17] and previous experiments[7,11] support the notion that highly localized plasmon modes are created by strong electromagnetic coupling between adjacent metallic nanorods or wires. The sharp TM plasmon peak at 357 nm is also evidence of the strong nature of the *s*-polarized electric field in the nanorod array.[18]

Figure 6 illustrates how an enhanced field trapped in the gap between nanorods is responsible for the high *s*-polarized SERS intensity. The nanorod array protrudes from the surface at a tilted angle, producing a three-dimensional nanorod lattice. The maximum electric field amplitude at the center of this three-dimensional lattice will be larger than the two-dimensional case of an electric field present between two nanorods on a planar surface due to increased nearest-neighbor dipole contributions. Although the rod−rod separation we measured (∼177 nm) is large compared to the conditions estimated by theory to produce optimum enhancements,[1,17] the lateral arrangement of the three-dimensional tilted nanorod lattice is likely to be an important component in the observed SERS anisotropy.

An additional factor in the SERS enhancements may be the nonuniform nature of the Ag nanorod cylinders produced by the oblique-angle vapor deposition method. The OAD method produces nanorods that deviate from an ideal cylindrical shape. These deviations include features as corrugations, needles, and bifurcations of the nanorods, see, e.g., Figure 1c and d. Such nanoparticle irregularities have been shown to generate SERS "hot spots" in the gaps between two adjacent nanoparticles, especially in the case of Y-junctions and bifurcated nanorods.[10]

Conclusions

We have shown that highly aligned Ag nanorod arrays produce a uniform lattice of high-aspect-ratio nanoparticles that gives an excellent SERS response.[13] The nature of the SERS polarization anisotropy observed for these substrates suggests that there is a strong electromagnetic coupling between adjacent nanorods, a position that is supported by previous theoretical calculations[17] and experiments.[7,11] We are, therefore, in a position to design substrates that can exploit this phenomenon for analytical applications.

Acknowledgment. Y.P.Z. and S.B.C. are thankful for the support from the NSF (ECS-0304340). S.S. and R.A.D. are supported by NIH grant EB001956.

References and Notes

(1) Xu, H.; Käll, M. *Chemphyschem* **2003**, *4*, 1001.
(2) Itoh, T.; Hashimoto, K.; Ikehata, A.; Ozaki, Y. *Appl. Phys. Lett.* **2003**, *83*, 5557.
(3) Itoh, T.; Hashimoto, K.; Ozaki, Y. *Appl. Phys. Lett.* **2003**, *83*, 2274.
(4) Käll, M.; Xu, H.; Johansson, P. *J. Raman Spectrosc.* **2005**, *36*, 510.
(5) Grand, J.; Lamy de la Chappelle, M.; Bijeon, J.-L.; Adam, P.-M.; Vial, A.; Royer, P. *Phys. Rev. B* **2005**, *72*, 033407.
(6) Jeong, D. H.; Zhang, Y. X.; Moskovits, M. *J. Phys. Chem. B* **2004**, *108*, 12724.
(7) Tao, A. R.; Yang, P. *J. Phys. Chem. B* **2005**, *109*, 15687.
(8) Brolo, A. G.; Addison, C. J. *J. Raman Spectrosc.* **2005**, *36*, 629.
(9) Brolo, A. G.; Arctander, E.; Addison, C. J. *J. Phys. Chem. B* **2005**, *109*, 401.
(10) Moskovits, M.; Jeong, D. H. *Chem. Phys. Lett.* **2004**, *397*, 91.
(11) Martinez, J. L.; Gao, Y.; Lopez-Rios, T.; Wirgin, A. *Phys. Rev. B* **1987**, *35*, 9481.
(12) Tao, A.; Kim, F.; Hess, C.; Goldberger, J.; He, R.; Sun, Y.; Xia, Y.; Yang, P. *Nano Lett.* **2003**, *3*, 1229.
(13) Chaney, S. B.; Shanmukh, S.; Zhao, Y.-P.; Dluhy, R. A. *Appl. Phys. Lett.* **2005**, *87*, 31908.
(14) Yang, W.-H.; Hulteen, J.; Schatz, G. C.; Van Duyne, R. P. *J. Chem. Phys.* **1996**, *104*, 4313.
(15) Norrod, K. L.; Sudnik, L. M.; Rousell, D.; Rowlen, K. L. *Appl. Spectrosc.* **1997**, *51*, 994.
(16) Bohren, C. F.; Huffman, D. R. *Absorption and Scattering of Light by Small Particles*; Wiley: New York, 1983.
(17) Garcia-Vidal, F. J.; Pendry, J. B. *Phys. Rev. Lett.* **1996**, *77*, 1163.
(18) Zou, S. L.; Janel, N.; Schatz, G. C. *J. Chem. Phys.* **2004**, *120*, 10871.